

# OBSERVATION OF CURRENT-DRIVEN FEATURES OF 2.5 MeV ION BUNCH WITH COMPLETE AND EFFICIENT 5D MEASUREMENTS AT THE SNS BEAM TEST FACILITY\*

K. Ruisard<sup>†</sup>, A. Aleksandrov, S. Cousineau, A. Hoover, A. Zhukov  
 Oak Ridge National Laboratory, Oak Ridge, TN 37830, USA

## Abstract

The SNS Beam Test Facility (BTF) research program is focused on detailed studies of beam distributions for medium-energy ion beams, with the goal of reconstructing realistic 6D bunch distributions to enable halo prediction. For complete characterization of the initial distribution, scan time scales exponentially with scan dimension. Currently, a full 6D measurement with about 10 points across most dimensions requires 24 hours. However, measurement of the 5D distribution  $f(x, x', y, y', w)$  can be done very rapidly using a hybrid slit/screen method. This approach requires approximately 4 hours to obtain at least 32 points/dimension, with very high resolution (0.5 keV) in the energy distribution. This presentation reports on the approach and results for 5D characterization of the initial RFQ-formed bunch. This includes higher-resolution views of previously reported transverse-longitudinal dependence and additional interplane dependencies that were not previously reported.

## INTRODUCTION

Precise, predictive modeling of high current hadron beams is difficult, due to the complexity of accelerator systems. This complexity is a result of beamline elements, as well as the beam distribution itself. This complexity limits model accuracy. Model/measurement discrepancies are often attributed to incomplete knowledge of the initial beam distribution (e.g., [1]). Work at the Spallation Neutron Source (SNS) Beam Test Facility (BTF) is focused on directly mapping the 6D distribution of the bunched beam after the RFQ. The goal of this work is to enable predictive modeling of downstream beam distributions with halo.

Full and direct 6D measurement allows reconstruction of a realistic, fully-correlated phase space without imposing assumptions on the shape of the distribution. The feasibility of 6D measurement was demonstrated in Ref. [2]. More recently, high resolution measurements in a 5D phase space allow more detailed views of the space-charge driven correlations in the BTF  $H^-$  bunch.

## MEASUREMENT APPROACH

A detailed description of the BTF is available in Ref. [3]. The system consists of an RF-driven  $H^-$  ion source, 65 keV LEBT and 402.5 MHz radiofrequency quadrupole (RFQ),

\* Notice: This manuscript has been authored by UT-Battelle, LLC, under contract DE-AC05-00OR22725 with the US Department of Energy (DOE).

<sup>†</sup> ruisardkj@ornl.gov

all identical to the components in the SNS front-end. This is followed by a 2.5 MeV MEBT (medium energy transport). This MEBT is much longer than the SNS design, contains no re-bunching cavities, and includes a 4 meter, 9.5-cell FODO line consisting of permanent magnet quadrupoles.

The BTF is equipped for full-and-direct measurement of the 6D phase space distribution  $f(x, x', y, y', \phi, w)$ . The 6D apparatus is described in Ref. [2]. To summarize here, the measurement apparatus consists of 3 vertical slits, a 90-degree dipole, 1 horizontal slit and a bunch shape monitor with a horizontal wire for secondary electron emission. In order to fully map the 6D space, the 4 slits and 1 wire are scanned in a 5D grid pattern. For each coordinate in 5D space, the phase distribution  $f(\phi)$  is measured instantaneously using a camera and viewscreen in the bunch shape monitor.

This is an inherently lengthy measurement, as a rectilinear scan with  $n$  points per dimension will record roughly  $n^5$  data points. (Only roughly, because one slit is "flying" and the number of points recorded during a pass varies). A recent 6D measurement on a  $10 \times 10 \times 32 \times 10 \times 258 \times 12$  grid in  $(x, x', y, y', \phi, w)$  coordinates required 24 hours of measurement time for beam at 5 Hz. Due to the high dimensionality, if the data rate were doubled the resolution would only improve by 15%.

Reducing scan dimension is a much more effective method to increase resolution. The geometry for a 5D phase space measurement is shown in Fig. 1. Here, 3 slits and a viewscreen are used to map the distribution  $f_{5D} = \int d\phi f(x, x', y, y', \phi, w)$ . Because this measurement takes advantage of both viewscreen axes, a 3D scan can make a complete mapping of the 5D space with  $n^3$  data points. Holding duration fixed and increasing scan resolution, a 5D scan should have  $n^{\frac{2}{3}}$  times more points per dimension. The

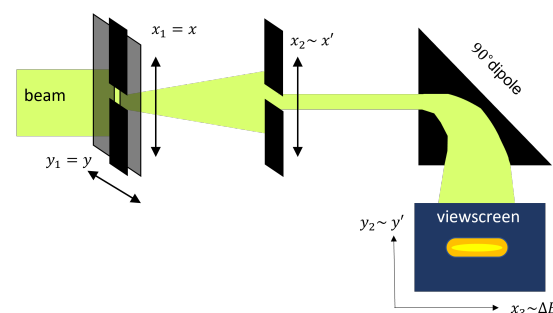


Figure 1: Geometry of 5D measurement apparatus, reproduced from Ref. [4].

scaling is actually stronger than this, closer to but not quite equal to factor  $n$  improvement, due to the flying slit.

The 5D data discussed here was collected over a duration of 7.6 hours on 7/15/2022 at  $26.73 \pm 0.06$  mA. This data was collected on a grid of  $43 \times 43 \times 43 \times 612 \times 512$  in slit coordinates  $(x_1, x_2, y_1, y_2, w)$ . The dimension  $y_1$  is sampled by the “flying slit” and has irregular spacing between points.

### Stability During Measurements

The stability of beam parameters pulse-to-pulse is critical to permit accurate reconstruction of bunch parameters. RMS variation of the beam current as recorded by a beam current monitor downstream of the RFQ is low, less than 0.3% with maximum variation of 1% during the scan duration.

Stability over long scan duration is also important, as drifts could dilute the phase space volume. Figure 2 illustrates the consistency of the long, high-dimensional scan with a more rapid, 2D phase space measurement. Two data sets, recorded 14 days apart, show excellent agreement. The slightly higher sensitivity of the 2D measurement (black contour) is due to the dependence of dynamic range on the number of slits inserted.

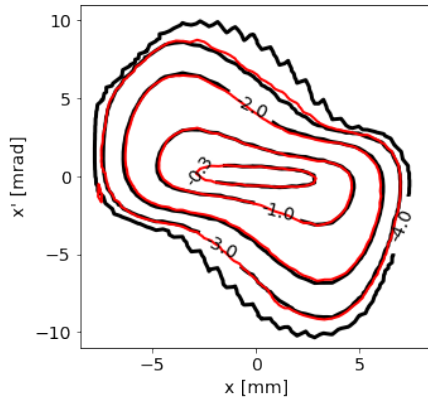


Figure 2: Comparison of 2D vertical phase space, using logarithmic-scale contours at the levels  $10^{-0.5}$ ,  $10^{-1}$ ,  $10^{-2}$ ,  $10^{-3}$ ,  $10^{-4}$  of peak density. The red contour is a projection of the 7.6-hour 5D measurement discussed in this paper. The black contour is the result of a 7.7 minute 2D phase space measured one week prior, on 7/1/2022.

### ANALYSIS

The measured data takes the form of a sequence of images of size  $512 \times 612$ , recorded for a distinct coordinate in the slit positions  $x_1, x_2, y_1$  (see annotations in Fig. 1). The  $y_1$  slit sweeps continuously across the beam. Between each sweep, the  $x_1$  and  $x_2$  slits are stepped in a grid pattern. At 5 Hz pulse repetition rate and 2.5 mm/s maximum sweep speed, the spacing between points in  $y_1$  coordinate is at most 0.5 mm.

To fully examine slice and projection views, the data must be converted from raw slit coordinates to phase space coordinates using matrix transformations. There are no quadrupole

fields between the first slit and the viewscreen. The transformations are:

$$x = x_1 \quad (1)$$

$$y = y_1 \quad (2)$$

$$x' = (x_2 - x_1)/L_1 \quad (3)$$

$$y' = (y_2 - y_1)/(L_1 + L_2 + \rho + L_3) \quad (4)$$

$$\frac{\delta p}{p} = \frac{1}{L_3 + \rho} \left( x_3 + \frac{L_3}{\rho} x - \left( \rho - \frac{(L_1 + L_2)L_3}{\rho} \right) x' \right) \quad (5)$$

where  $L_1 = 0.95$  meters is slit-slit spacing,  $L_2 = 0.57$  meters is slit-dipole drift length,  $L_3 = 0.13$  meters is dipole-screen drift length, and the  $90^\circ$  dipole bending radius is  $\rho = 0.356$  meters.

The slit actuators give a very precise reading of slit position in millimeters that is synchronized with the pulse timing. The size of the camera pixels,  $0.03 \pm 0.002$  mm/pixel, is calibrated against the upstream slit positions. This can be done using the fact that the vertical phase space distribution  $f(y, y')$  should be the same whether measured in a slit-slit or slit-screen configuration.

Use of the viewscreen could support a minimum energy resolution of 0.3 keV (given the field of view and camera resolution). This is slightly below the resolution limit dictated by finite slit sizes (0.2 mm) for resolving  $x_1$  and  $x_2$ , which is estimated to be 0.4 keV in [5]. The vertical momentum coordinate  $y'$  is also measured at a very high resolution. In this case the resolution limit is dominated by the width of the upstream slit  $y_1$ , which contributes a point spread of 0.1 mrad. This is halved from the slit-slit geometry, as the slit-screen distance is more than twice the slit-slit distance.

For the data shown here, the camera resolution is reduced by a factor of 9 to reduce array size. This is still an improvement from the 6D scan, which most recently ran with steps of 14keV and 2mrad in  $w$  and  $y'$ .

After the transformations in Equations 1 - 5 are applied, the resulting density is linearly interpolated onto a regular grid in the phase space coordinates. This interpolation is done in two parts; first every 3D slice  $f(y_1, y_2, x_3)$ , which is a sequence of images  $f(y_2, x_3)$  recorded during one pass of flying slit  $y_1$ , is transformed to  $f(y, y', x_3)$ . In this step, the irregularly-spaced  $y_1$  points are interpolated to regular spacing in  $y$ . Second, each 3D slice  $f(x_1, x_2, x_3)$  is transformed to  $f(x, x', w)$  and interpolated onto a regular grid. The data shown here is interpolated to a grid of size  $45 \times 45 \times 45 \times 50 \times 80$  in units  $(x, x', y, y', w)$ .

### RESULTS

Some views of the measured 26 mA distribution are shown in Figs. 3 and 4. In both figures, frame (a) shows a 2D slice through the core of the 5D distribution, while frame (d) shows a fully-projected view. Frames (b) and (c) show slices through a 4D and 3D projection, respectively. The fully projected views suggest that there are no correlations between the planes. In contrast, the high-dimensional views reveal dependencies between the coordinates, in the form of

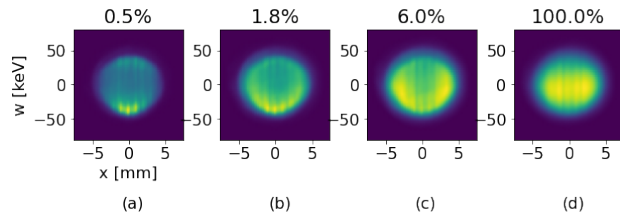


Figure 3: Distribution  $f(x,w)$  for different slices through the beam core. The percentage of signal within the slice is indicated. (a) Particles are constrained by  $x' = 0 \pm .1\text{mrad}$ ,  $y = 0 \pm .1\text{mm}$ ,  $y' = 0 \pm .1\text{mrad}$ , (b) by  $y = 0 \pm .1\text{mm}$ ,  $y' = 0 \pm .1\text{mrad}$ , (c) by  $y = 0 \pm .1\text{mm}$ . (d) is fully-projected.

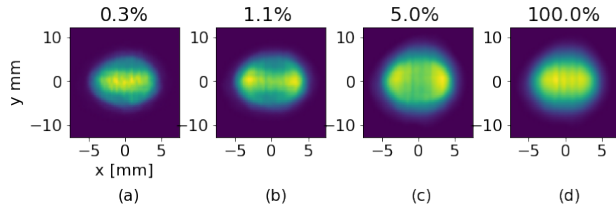


Figure 4: Distribution  $f(x,y)$  for different slices, constrained by (a)  $x' = 0 \pm .1\text{mrad}$ ,  $y' = 0 \pm .1\text{mrad}$ ,  $w = 0 \pm 0.4\text{keV}$  (b) by  $y' = 0 \pm .1\text{mrad}$ ,  $w = 0 \pm 0.4\text{keV}$  (c) by  $w = 0 \pm 0.4\text{keV}$ . (d) is fully-projected.

hollowing in the longitudinal and horizontal planes. There is an  $x, y$  asymmetry, as no vertical hollowing is observed.

The longitudinal hollowing has previously been reported and is shown to be dependent on bunch charge [2]. The transverse hollowing is a more recent observation enabled by the very fine transverse resolution obtained in the 5D measurement. Simulation studies suggest the transverse hollowing is also space-charge driven. This is supported by preliminary measurement at three different beam currents, summarized in Fig. 5.

Unlike the SNS MEBT, the BTF does not contain re-buncher cavities and the beam rapidly debunches after the RFQ. At the measurement location, there is a large linear  $w, \phi$  correlation. As a result, examining slices in the energy distribution also has the effect of localizing particles in phase. For example, the slice at  $w = 0 \pm 0.4\text{keV}$  will only contain particles within a spatial range of  $\phi = 0 \pm 5^\circ$ .

The 5D measurement does not include any information about the phase distribution. However, due to the large correlation we expect that at the measurement location, the 3D spatial distribution  $f(x, y, \phi)$  will look very similar to  $f(x, y, w)$ . Frame (c) in both Figs. 3 and 4, which show cross-sections of the 3D distribution  $f(x, y, w)$ , suggest that the beam is spatially hollow at this point in the transport line. This means that the peak density at the beam core is lower than might be assumed by examining only full projection views.

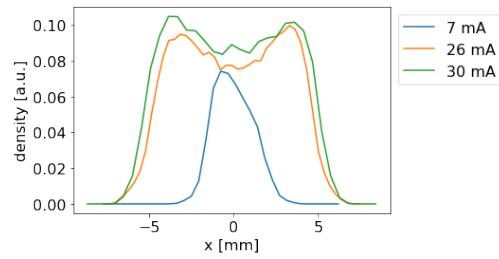


Figure 5: 1D distributions of a slice through the 3D projection:  $f_{1D}(x) = \int d\phi dx' dy' f_{6D}(x, x', y = 0, y', \phi, w = 0)$ . This captures the hollowing visible in Fig. 4, frame (c). The data shown here at 26 mA RFQ output is compared to two other 5D datasets at 30 mA and 7 mA. The difference in current values is due to different ion source output.

## DISCUSSION AND OUTLOOK

This paper discussed the results of measurement of the 5D distribution  $f_{5D} = \int d\phi f(x, x', y, y', \phi, w)$  of the  $H^-$  ion bunch produced by the RFQ in the SNS BTF. Much higher resolution is possible in 5D compared to 6D measurements, sufficient to resolve the high dimensional distribution. We observe there is longitudinal hollowing visible in the transverse beam core, as well as transverse (horizontal) hollowing in the longitudinal core. These correlations are understood to be a result of space charge forces.

While the 5D measurement is useful for visualizing the beam distribution, there is not sufficient information to seed macroparticles for simulation. Future efforts will focus on increasing 6D resolution by reducing scan dimension. A 2D bunch shape monitor[6] capable of measuring  $f(\phi, w)$  instantaneously opens up the possibility of using 4D scans to fully map the 6D phase space. Alternative strategies include inferring the missing dimension (phase) from a 5D measurement, as proposed in [7].

## ACKNOWLEDGEMENTS

This work relies on expertise and support from SNS Operations and the Research Accelerator Division at ORNL, particularly from Beam Instrumentation, Front End Systems, and Mechanical Engineering groups. This material is based upon work supported by the U.S. Department of Energy, Office of Science, Office of High Energy Physics. This manuscript has been authored by UT- Battelle, LLC under Contract No. DE-AC05-00OR22725 with the U.S. Department of Energy. This research used resources at the Spallation Neutron Source, a DOE Office of Science User Facility operated by the Oak Ridge National Laboratory.

## REFERENCES

- [1] J. Qiang, P.L. Colestock, D. Gilpatrick, H. V. Smith, T. P. Wangler, and M. E. Schulze, "Macroparticle simulation studies of a proton beam halo experiment," *Phys. Rev. Spec. Top. Accel. Beams*, vol. 5, no. 12, p. 124201, 2002. doi:10.1103/PhysRevSTAB.5.124201

- [2] B. Cathey, S. Cousineau, A. Aleksandrov, and A. Zhukov, "First Six Dimensional Phase Space Measurement of an Accelerator Beam," *Phys. Rev. Lett.*, vol. 121, no. 6, p. 064 804, 2018. doi:10.1103/PhysRevLett.121.064804
- [3] Z. Zhang, S. Cousineau, A. Aleksandrov, A. Menshov, and A. Zhukov, "Design and commissioning of the Beam Test Facility at the Spallation Neutron Source," *Nucl. Instrum. Methods Phys. Res. Sect. A*, vol. 949, p. 162 826, 2020. doi:10.1016/j.nima.2019.162826
- [4] K. Ruisard, A. V. Aleksandrov, S. M. Cousineau, A. M. Hoover, and A. P. Zhukov, "Model / measurement comparison of the transverse phase space distribution of an RQF-generated bunch at the SNS," presented at NAPAC'22, Albuquerque, NM, USA, Aug. 2022, paper WEYE5.
- [5] K. Ruisard, A. Aleksandrov, S. Cousineau, A. Shishlo, V. Tzoganis, and A. Zhukov, "High dimensional characterization of the longitudinal phase space formed in a radio frequency quadrupole," *Phys. Rev. Accel. Beams*, vol. 23, no. 12, p. 124 201, 2020. doi:10.1103/PhysRevAccelBeams.23.124201
- [6] S. Kutsaev, R. Agustsson, A. Aleksandrov, O. Adonyev, A. Moro, and K. Taletski, "Advanced focusing system for secondary electrons in a bunch shape monitor," *Nucl. Instrum. Methods Phys. Res. A*, vol. 1019, p. 165 846, 2021. doi:10.1016/j.nima.2021.165846
- [7] A. M. Hoover, K. Ruisard, A. V. Aleksandrov, S. M. Cousineau, and A. P. Zhukov, "Measurements of the five-dimensional phase space distribution of an intense ion beam," presented at NAPAC'22, Albuquerque, NM, USA, Aug. 2022, paper FRXD3.